Building a Tensor Framework for the Analysis and Classification of Steady-State Visual Evoked Potentials in Children

Eli Kinney-Lang, Ahmed Ebied, and Javier Escudero
School of Engineering, Institute for Digital Communications
University of Edinburgh
Edinburgh, United Kingdom EH9 3FG
Email: e.kinney-lang@ed.ac.uk

***Abstract*—Steady-state visual evoked potentials (SSVEP) are one of several underlying signals used in various electroencephalography (EEG) based applications, including brain-computer interface (BCI) technology. Through oscillating visual stimulus at distinct frequencies, an SSVEP can be detected by EEG at occipital electrodes on the scalp, with distinct visual stimuli representing distinct choices. Rapid, accurate detection and classification of these signals is crucial for real-time analysis in SSVEP-based applications. However, signal analysis and interpretation of SSVEP events may be hindered in children due to the significant variability in electrophysiological signals throughout development. Recently, multi-way tensors have been shown capable of exploiting higher-order interactions present in the naturally multi-dimensional EEG data. Using tensors as tools to identify latent structures between varying maturational signals thus may provide a potential solution for rapid classification of SSVEP signals in children at different developmental stages. The presented methodology builds upon previous tensor-based SSVEP analysis and extends it for the first time to developing paediatric populations. Results from a binary SSVEP classification task of $n = 40$ children age 8-11 are reported to be significantly greater than chance, at 67-74% accuracy across multiple training and testing blocks. The findings support that tensor decomposition could provide flexible advantages capable of accommodating developmental differences across children and lay groundwork for future tensor analysis in SSVEP-based applications, like BCIs.**

***Index Terms*—multi-way analysis, tensor analysis, SSVEP, child development, brain-computer interface**

I. Introduction

Brain-computer interfaces (BCI) are an emerging technology, offering a means for non-muscular control of output devices, like computers, through direct analysis of brain signals and patterns [1]. A common signal exploited in BCI technology is the steady-state visual evoked potential (SSVEP) [2], [3], in which several selection options are associated with visual objects oscillating at distinct frequencies [2]. These oscillations cause a synchronization of the natural brain rhythms over the occipital region of the brain, and can be detected using scalp electrodes via electroencephalography (EEG). Such signals are then associated with specific selection choices, e.g. letters on a screen [2].

The direct nature of elucidating SSVEP signals is enticing for building BCI technologies for complex populations, like maturing children. Considering the scope of structural and functional changes associated with development, designing appropriate BCIs for children presents multiple challenges [4], [5]. One hurdle facing paediatric BCIs is the ongoing progression of electrophysiological signals and networks identified by the EEG throughout development [6], [7]. Previous work on SSVEP-based paediatric BCIs demonstrated inherent age-specific responses in SSVEP-based BCI tasks [8]. Results indicated a link between the brain's ability to synchronize spontaneous and steady-state evoked oscillations with its maturation throughout childhood [8], [9]. A potential avenue to incorporate these inherent maturational differences within EEG signals is through the use of multi-way tensor analysis [4], [10], by means of maintaining and investigating the naturally occurring higher-order structure of EEG data across developing subjects.

Tensor analysis extends traditional matrix (two-way) analytic techniques to its multi-linear correlate, thereby allowing the simultaneous analysis of three or more domains (also called modes or ways) of data [3], [11]. For example, tensor analysis of EEG data maintains the inherent relationships between the $[Spatial]$ (i.e. channel),$[Temporal]$ and $[Frequency]$ domains of the EEG, whereas matrix-based analysis would only inform on some two-combination of those domains [3]. Thus higher-order EEG structural information which is typically lost in matrix analysis is maintained, thereby providing further insight into the latent relationships within the EEG data [3].

Exploiting advantages gained by tensor analysis has been previously demonstrated as an effective tool in SSVEP-based BCIs for adults [3], [12], [13]. Additionally, tensor-based BCI results have established tensors as a potential tool for avoiding the subject-specific calibration in BCI classification [14]. Reducing the calibration time for a subject thus leads to improved BCI set-up speed and increases its child-friendly nature [4]. However, little previous work has been done to adapt BCI paradigms specifically to children [4], [5]. Therefore, this paper outlines for the first time initial steps in adjusting SSVEP signal processing techniques common in BCI paradigms to accommodate paediatric populations. The work proposes an effective tensor analysis scheme to classify binary SSVEP selection tasks in children, and demonstrates

ISBN 978-90-827970-1-5

its potential using a publicly available dataset.

II. Materials and Methods

This paper follows tensor notation defined in [15]. Summary of key notation includes calligraphic upper case letters ($\mathcal{A}$) as tensors, boldface upper case letters ($\mathbf{A}$) as matrices, lower case ($\mathbf{a}$) as vectors, $\mathbf{A}^{(i)}$ as the ith-mode matrix of a tensor, with operations $\circ$ as the vector outer product, $\otimes$ as the Kronecker tensor product, $\odot$ as the Khatri-Rao (column-wise Kronecker) product and † as the Moore-Penrose pseudo inverse.

Dataset and pre-processing

Data in this study was derived from the publicly available EEG dataset provided by the Child Mind Institute [16]. EEG data was recorded from a high-density 129-electrode hydrocel EEG cap for $n = 44$ children and pre-processed as described in [16]. Multiple recordings were taken for each child covering several resting and task-oriented paradigms. In particular, the *Contrast Change Paradigm* (CCP) was used for SSVEP data collection. The CCP design allowed isolation of several specific brain processing phenomena, including an information encoding phase reflected by an induced SSVEP at 20 and 25 Hz for left and right object selection, respectively [16]. The subject was instructed to pay attention to one of the objects based on increasing contrast and push the corresponding left/right button. Full details on the CCP can be found in [16]. A random set of 24 distinct trials of selection (12 left, 12 right) were run in a block of the CCP, and each child attempted to complete 3 CCP blocks. Of the available data, $n = 40$ children were able to complete at least 2 of the 3 blocks with good responses, and were therefore selected for classification analysis in this paper.

Data for the SSVEP was processed as follows. For each subject, a trial was defined as the 2 seconds prior to a button press. Spectral power in the frequency range 17-30Hz was calculated for each trial across 18 occipital channels using the Fieldtrip toolbox for MATLAB [17]. Trials which had poor EEG channel interpolation and/or abnormally high amplitude variance (i.e. a 10-fold difference) were excluded from analysis. The SSVEP data was labelled as either left or right, based on the corresponding button press.

Tensor construction, decomposition and modelling

From the clean SSVEP data, a 4-mode tensor $\mathcal{X}$ was built with domains $[Trial] \times [Spatial] \times [Frequency] \times [Subject]$. The $[Trial]$ domain was structured such that the first 12 elements were left-trials, followed by 12 right-trials. This removed the randomized left/right trial order in any given CCP block, allowing for the $[Subject]$ domain to be compared in the constructed tensor. Furthermore, the $[Subject]$ domain was arranged from youngest to oldest to account for potential developmental differences associated with age, similar to [10].

The constructed tensor $\mathcal{X}$ was then decomposed into a 3-component model using Parallel Factor Analysis (PARAFAC) [15], [18] via the N-way and Tensorlab toolboxes for MATLAB [19], [20]. The PARAFAC decomposition models a tensor $\mathcal{X}$ as the sum of component rank-one tensors, with

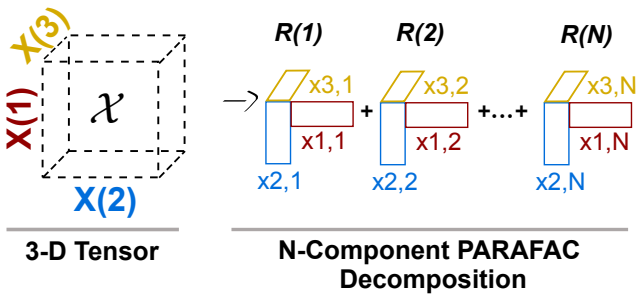

Fig. 1. PARAFAC decomposition for a generic 3-way tensor $\mathcal{X}$ into N component matrices (R). Only components of the same color interact across the N domains (i.e. $x_{1,1}$ with $x_{1,2}$ etc.).

components interacting on a strict 1:1 basis between domains as in Figure 1. Equation (1) shows a three component decomposition for our 4-mode tensor $\mathcal{X}$ with domain matrices $\mathbf{A}^{(n)}$ and elements $a_{ij}^{(n)}$, $n = 1, 2, 3, 4$ as:

$$\mathcal{X} = \sum_{r=1}^{R=3} a_r^{(1)} \circ a_r^{(2)} \circ a_r^{(3)} \circ a_r^{(4)} \tag{1}$$

Non-negativity was enforced in the $[Trial], [Spatial]$ and $[Subject]$ domains, with orthogonality imposed on the $[Frequency]$ domain. The non-negativity constraints improved interpretation of the resulting component matrices, while orthogonality guaranteed linear independence between factors representing the distinct frequency SSVEP peaks at 20 and 25 Hz. A 3-component decomposition was selected so distinct factors for the two SSVEP signals of interest could be uniquely described, with the third factor accounting for any other variability or irrelevant noise. Explained variance for the constrained 3-component model was approximately 41% as compared to the 43% explained variance without constraints. Using more components for decomposition did not significantly improve the explained variance of the model (5-components had 42% explained variance), and introduced a greater risk of overfitting in the $[Subject]$ domain [10]. Using fewer than 3 components would mean the PARAFAC model could not separate the desired signals distinctly from each other and noise.

Projection and Classification

For each CCP-block of data, the whole block was designated as either training or testing. For training, the CCP SSVEP data was analyzed using the above tensor analysis, providing resultant component matrices, $\mathbf{X}^{(n)}$ in each domain. Of the $n = 40$ children from pre-processing, unique subsets of $n = 34, 36, 35$ children completed CCP-blocks 1, 2 and 3, respectively. Testing consisted of binary classification on each trial individually for each subject into 'left' or 'right' categories. This was similar to work done in [14], where an auditory BCI distinguished between two tones at different frequencies. Properties of new trials were compared to the target tones based on a leave-one-out average response to the tones over all other trials available. In the present work, in lieu of grand averaging, new weights are estimated through direct projection as outlined in [10], [21], [22] in order to

ISBN 978-90-827970-1-5 © EURASIP 2018

maintain as much information as possible. The key steps in estimating the new weights via direct projection are included here for clarity. Full details can be found in [22].

The tensor $\mathcal{X}$ was unfolded along the component $[Subject]$ domain $\mathbf{X}^{(4)}$, to define a new-subject encoding matrix ($\mathbf{W}$):

$$\mathbf{W} = ([\mathbf{X}^{(3)} \odot \mathbf{X}^{(2)}]^T)^{\dagger} \quad (2)$$

where $\mathbf{X}^{(n)}$ for $n = 2, 3$ holds the estimated interactions between the $[Spatial]$ and $[Frequency]$ component domains, respectively. Since each trial is independently classified (as would be expected in a real BCI setting), information from the $[Trial]$ domain could not be explicitly included in $\mathbf{W}$. This is due to direct projection requiring 1:1 matched elements across each projected domain, while a 1:24 ratio exists for the given $[Trial]$ domain. However, due to the strict nature of how components interact across domains in PARAFAC, the estimated interactions in $\mathbf{W}$ have inherited properties corresponding to $[Trial]$ (and $[Subject]$) domain structures, as outlined in Figure 2. Then, any new incoming $[Subject]$ EEG data can be multiplied by the encoding matrix $\mathbf{W}$ in order to estimate the new data's $[Spatial]$ and $[Frequency]$ weights.

III. Results

Tensor analysis was performed across the six combinations of the 3-block CCP data (e.g. Block1-Train, Block2-Test; Block1-Train, Block3-Test; etc.). For each, trials for every subject were selected randomly for testing via direct projection. New subjects from the testing tensor $\mathcal{Y}$ were then projected onto the common interactions held by $\mathbf{W}$ to estimated weights w_y using Equation (2). These weights informed on the new subject's status with respect to the extracted tensor components. Knowing which components in the PARAFAC model reflected the noise, left and right SSVEP signals (as seen in the bottom-left $[Frequency]$ domain panel of Figure 2) permitted each given trial to be classified as 'left' or 'right' based on the highest corresponding component weight in w_y. Ground truth was taken to be the actual button press for the trial. Left, right and total accuracy were calculated for each child based on the mean across all trials. Figure 3 shows a box-plot of resulting accuracy across all children and all trials for each CCP-block combination. Classification above 66.7% is considered to be significantly greater than chance at $p = 0.05$ for a binomial distribution of 24 trials with equal classification probability.

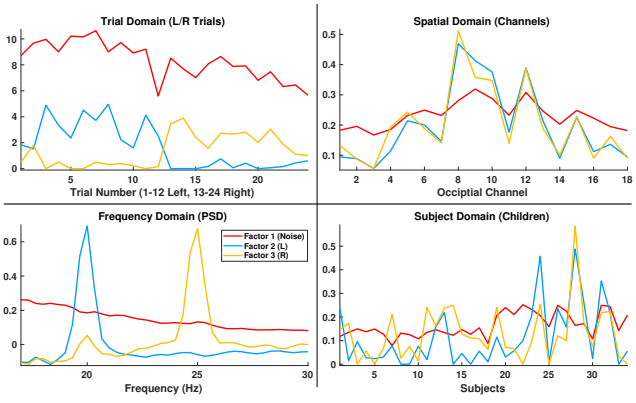

Fig. 2. Example of a constrained 3-component SSVEP decomposition from the 4-mode CCP of Block 1. In each component domain, direct interaction occurs only between the same factors, e.g. red relates to red across all panels. In the example, the $[Frequency]$ domain captures noise and target SSVEP signals at 20,25 Hz in the red, blue and yellow factors respectively. Similar decompositions can be found for CCP blocks 2 and 3.

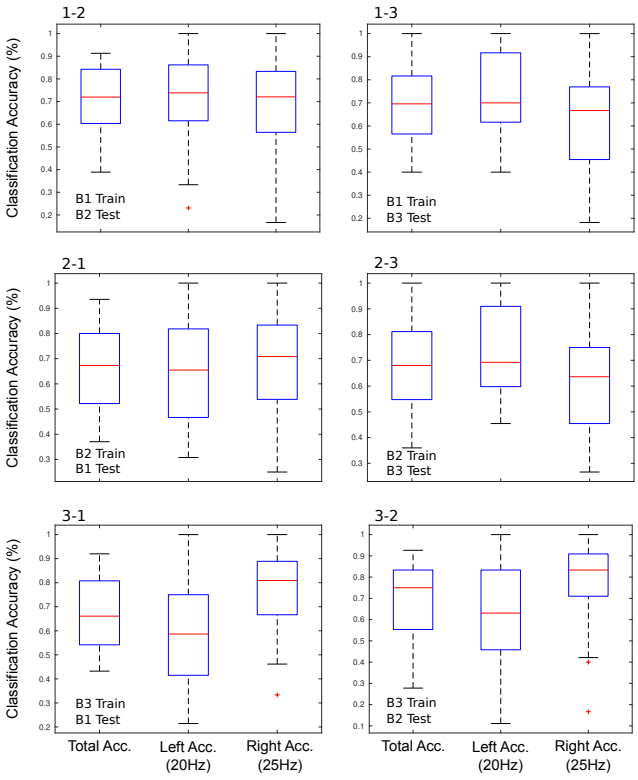

Fig. 3. Box-plot results of the average total, left-target and right-target accuracy across subjects and trials. Each panel shows individual train-test block accuracy across all children who completed the given CCP block ($n = 34, 36, 35$ for blocks 1,2 and 3, respectively). Total accuracy was relatively consistent across CCP combinations, at approximately 70%. Outlier subjects are indicated beyond the box-plot range by a + symbol.

Figure 4 illustrates the raw power spectrum for occipital channels in two representative children during left-selection SSVEP (20 Hz) tasks. The results include a subset of 6 left-trials and an 'overall mean' comparison between prototypical 'good SSVEP' and 'poor SSVEP' response children.

The results indicate the extracted tensor components are relatively robust for classification, even when the target signal is not immediately discernible like in Child 2 of Figure 4. For the example children, the proposed tensor classification scheme was 100% accurate in predicting any given trial as 'left' in Child 1, and 64% accurate for Child 2. By utilizing information from both $[Trial]$ and $[Subject]$ domains in the original training tensor, the PARAFAC model decomposition can implicitly underscore which trials (and subjects) are representative (or not) of the signals of interest. This is evident when comparing the loading contributions for the left-selection (20 Hz) signal of Child 1 and Child 2 in the $[Subject]$ domain panel of Figure 2. Child 1 contributes approximately 15x more to defining the extracted left-selection

ISBN 978-90-827970-1-5 © EURASIP 2018

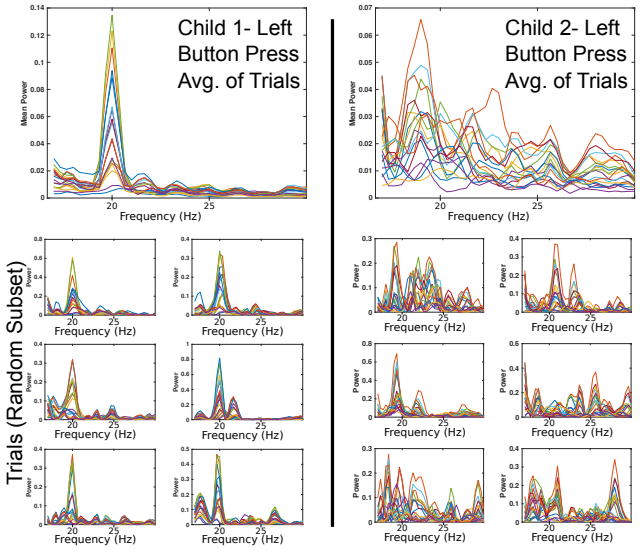

Fig. 4. Comparison of power at occipital channels between two children during left-selection (20 Hz) tasks in CCP Block 1. The left-selection SSVEP task would expect synchronization at 20 Hz. The left column shows a representative child with a clear left-selection SSVEP signal, while the right column shows a child with less clear left-selection SSVEP signals. The average spectral power across trials for each channel is shown in the top panel of both columns, with the smaller panels illustrating a random subset of the individual trials. Left-task classification accuracy for Child 1 was 100% and for Child 2 was 64% using the proposed tensor analysis.

component compared to Child 2 ($l = 0.24$ for Child 1, $l = 0.016$ for Child 2). Despite this large disparity, left-selection trials from Child 2 were still correctly identified approximately 64% of the time. This indicates that accuracy rates for signals of interest can largely be maintained for noisy, unclear trials.

Also of interest is that significant correlation exists between a child's contribution in a given decomposition and their reported classification accuracy score (Pearson's correlation, with p-values $p = 0.0055, p = 0.0002$ for total accuracy of left and right trials, respectively). However, this correlation held only when considering the signals of interest. No correlation was found between contribution to noise and any accuracy (with p-value, $p = 0.9895$). Correlation was calculated only for children common across all CCP Blocks.

IV. Discussion

The results from this study outline a tensor analysis scheme for binary classification which is capable of analyzing SSVEP data from children using direct projection. Through projection, the need for a subject-specific calibration step is removed. This reduces some of the set-up and calibration down time associated with traditional BCI tasks, and would thereby improve the user-experience for children [4]. Additionally, through isolating 'noise' into a single component, the tensor analysis is able to minimize the impact of continually developing electrophysiological states present throughout childhood [4], [23]. Finally, by including a $[Trial]$ domain, tensor analysis has huge potential for paediatric use because it can emphasize the trials in which a child does well, while minimizing the overall impact of failed, aborted or unsuccessful trials. This has strong implications in BCI paradigms, as children are more likely to abort or fail a task than adults [4].

The tensor analysis showed significant classification capabilities despite potential differences in development between the children. Of note, by ordering the $[Subject]$ domain to be increasing in age from 8-11 years old, general developmental information can be elucidated. For example, it appears that the latter half of subjects in Block 1 (seen in bottom right panel of Figure 2) holds the largest contributions to each component. In Block 1, subjects 1-17 were age 8-9, while subjects 18-34 were age 10-11. In this regard, contributions to components from the older children trended towards being more dominant (especially regarding the noise factor component) than younger children. From a developmental point-of-view, this indicates that the individual children who performed best (i.e. contributed most significantly to the PARAFAC component model) were, unsurprisingly, often the older children (i.e. the latter half of the $[Subject]$ domain in Figure 2). This can be seen clearly by Child 24, Child 28 and Child 31 in Figure 2 for left-selection task contribution (blue factor).

However, not all of the older children contributed more than the younger subjects. This highlights a few important developmental considerations in the results. First, the child's chronological age may not necessarily reflect their developmental state in its entirety. Second, by emphasizing children (and trials) which contributed most to target signals of interest (e.g. 20/25 Hz SSVEP signals) as well as identifying which children were mainly dominated by non-target signals (e.g. noise), the tensor analysis scheme can capture latent information on the developmental state of the children. To this end we postulate that the children ahead (behind) in development are reflected by larger (smaller) contributions to the tensor components. Then, if we consider the strong correlation between relative component contribution in the PARAFAC model and the classification accuracy, tracking the development of a child across sessions/interventions/therapies may be possible using the classification accuracy as a guide. This idea could be explored further in future investigations.

Given the simple nature of the classification, i.e. taking whichever new weight w_y is largest, the proposed tensor analysis scheme could be extended easily to decompositions with more than 2 target signals. Additionally, as classification is based on a rapid matrix multiplication of new subject trials by the encoding matrix, the proposed work could be readily introduced into real-time BCI systems. The computational complexity required for such endeavours would be relatively low. The major computational bottleneck occurs during the decomposition step, which could be done 'offline', prior to the 'online' classification element. The specific computational complexity would depend on the algorithm used (see [24] for details), but using tools like Tensorlab provides linear complexity in the decomposition algorithm [20]. The 'online' complexity is trivial, as the direct projection required for the classification element only requires simple matrix multiplication. Demonstrating the proposed tensor framework for these applications are another avenue for future work.

ISBN 978-90-827970-1-5 © EURASIP 2018

The presented work has some limitations to consider. When designating a specific trial as 'left' or 'right', the recorded button pressed was considered to be the ground truth. However, it is possible that some children may have focused on one object (left or right) and accidentally pressed the other button. As the analysis is based on a public dataset, and minimal direct oversight was given for each trial analyzed, it is possible some trials could have suffered from this discrepancy. However, the effect of such an error is likely to be small considering that the decomposition results provide flexibility in the $[Trial]$ domain for contributions to left/right components. With the significant classification results reported, the overall tensor analysis scheme remains quite promising.

Additionally, the public dataset used for analysis in this paper was not necessarily developed with the intent of SSVEP analysis and classification. However, the EEG task paradigm was designed in such a way that the relevant information was available for us to pose the questions and analysis presented in this paper. Subsequent investigations could expand upon this preliminary work through demonstrating its validity in an actual SSVEP-BCI setting.

V. Conclusion

This paper outlined a tensor analysis structure for classifying SSVEP signals of interest from a paediatric EEG dataset. The work demonstrated how a 4-mode tensor with domains $[Trial]\times[Spatial]\times[Frequency]\times[Subject]$, could be utilized for direct SSVEP classification between two trial categories, 'left' and 'right'. The 4-D tensor was modelled using a constrained 3-component PARAFAC decomposition, where orthogonality constraints guaranteed independence of the SSVEP signals of interest. Extracted components from the decomposition were used to define an encoding matrix for projecting new subjects (and new trial) data onto the latent structural interactions found in the training tensor. Results found left/right trial classification was approximately 70% accurate across combinations of training and testing blocks. Additionally, the tensor analysis was shown to be suitable even in children with extremely noisy trials. Exploiting the properties inherent in tensor analysis thus may provide a beneficial framework with boons for paediatric focused SSVEP analysis, e.g. in SSVEP-based BCI. Advantages via the outlined tensor framework includes the potential for dealing with varying noise across a developmental range of children, thereby accounting for varying states of development across children. Additionally, the tensor scheme offers a means for rapid classification without a subject-specific calibration phase improving suitability for paediatric subjects. Together, these results demonstrate tensor analysis as a promising tool for paediatric SSVEP-analysis applications.

Acknowledgements

The authors would like to thank the Child Mind Institute for the publicly available data, and thank the children and families who partook in the study.

References

[1] J. R. Wolpaw, "Brain-computer interfaces as new brain output pathways." *J. Physiol.*, vol. 579, no. 3, pp. 613–619, 2007.

[2] L. F. Nicolas-Alonso and J. Gomez-Gil, "Brain computer interfaces, a review." *Sensors (Basel).*, vol. 12, no. 2, pp. 1211–79, 2012.

[3] A. Cichocki *et al.*, "Noninvasive BCIs: Multiway Signal-Processing Array Decompositions," *Computer (Long. Beach. Calif).*, vol. 41, no. 10, pp. 34–42, Oct. 2008.

[4] E. Kinney-Lang, B. Auyeung, and J. Escudero, "Expanding the (kaleido)scope: exploring current literature trends for translating electroencephalography based braincomputer interfaces for motor rehabilitation in children," *J. Neural Eng.*, vol. 13, no. 6, p. 061002, 2016.

[5] E. Mikoajewska and D. Mikoajewski, "The prospects of brain computer interface applications in children," *Cent. Eur. J. Med.*, vol. 9, no. 1, pp. 74–79, 2013.

[6] T. Gasser *et al.*, "Development of the EEG of school-age children and adolescents. I. Analysis of band power," *Electroencephalogr. Clin. Neurophysiol.*, vol. 69, no. 2, pp. 91–99, Feb. 1988.

[7] P. J. Marshall, Y. Bar-Haim, and N. A. Fox, "Development of the EEG from 5 months to 4 years of age," *Clin. Neurophysiol.*, vol. 113, no. 8, pp. 1199–1208, 2002.

[8] J. Ehlers *et al.*, "Age-specific mechanisms in an SSVEP-based BCI scenario: evidences from spontaneous rhythms and neuronal oscillators." *Comput. Intell. Neurosci.*, vol. 2012, p. 967305, 2012.

[9] A. Birca *et al.*, "Maturational changes of 5Hz SSVEPs elicited by intermittent photic stimulation," *Int. J. Psychophysiol.*, vol. 78, no. 3, pp. 295–298, Dec. 2010.

[10] E. Kinney-Lang *et al.*, "Elucidating age-specific patterns from background electroencephalogram pediatric datasets via PARAFAC," in *2017 39th Annu. Int. Conf. IEEE Eng. Med. Biol. Soc.* IEEE, Jul. 2017, pp. 3797–3800.

[11] T. G. Kolda and B. W. Bader, "Algorithm 862: MATLAB tensor classes for fast algorithm prototyping," *ACM Trans. Math. Softw*, vol. 32, no. 4, pp. 635–653, 2006.

[12] H. Ji *et al.*, "EEG Classification for Hybrid Brain-Computer Interface Using a Tensor Based Multiclass Multimodal Analysis Scheme," *Comput. Intell. Neurosci.*, vol. 2016, pp. 1–15, 2016.

[13] H. Wang *et al.*, "Discriminative Feature Extraction via Multivariate Linear Regression for SSVEP-based BCI," *Neural Syst. Rehabil. Eng. IEEE Trans.*, vol. PP, no. 99, p. 1, 2016.

[14] R. Zink *et al.*, "Tensor-based classification of an auditory mobile BCI without a subject-specific calibration phase," *J. Neural Eng.*, vol. 13, no. 2, 2016.

[15] T. G. Kolda and B. W. Bader, "Tensor Decompositions and Applications," *SIAM Rev.*, vol. 51, no. 3, pp. 455–500, 2008.

[16] N. Langer *et al.*, "A resource for assessing information processing in the developing brain using EEG and eye tracking," *Sci. Data*, vol. 4, p. 170040, Apr. 2017.

[17] R. Oostenveld *et al.*, "FieldTrip: Open source software for advanced analysis of MEG, EEG, and invasive electrophysiological data," *Comput. Intell. Neurosci.*, vol. 2011, 2011.

[18] R. a. Harshman, "Foundations of the PARAFAC procedure: Models and conditions for an explanatory multimodal factor analysis," *UCLA Work. Pap. Phonetics*, vol. 16, no. 10, pp. 1– 84, 1970.

[19] C. A. Andersson and R. Bro, "The N-way Toolbox for MATLAB," *Chemom. Intell. Lab. Syst.*, vol. 52, no. 1, pp. 1–4, 2000.

[20] N. Vervliet, O. Debals, and L. De Lathauwer, "Tensorlab 3.0 - Numerical optimization strategies for large-scale constrained and coupled matrix/tensor factorization," in *Conf. Rec. - Asilomar Conf. Signals, Syst. Comput.* IEEE, nov 2017, pp. 1733–1738.

[21] J. Escudero *et al.*, "Multiscale entropy analysis of resting-state magnetoencephalogram with tensor factorisations in Alzheimer's disease," *Brain Res. Bull.*, vol. 119, pp. 136–144, Oct. 2015.

[22] E. Kinney-Lang *et al.*, "Tensor-driven extraction of developmental features from varying paediatric EEG datasets," *J. Neural Eng.*, may 2018.

[23] S. J. Segalowitz, D. L. Santesso, and M. K. Jetha, "Electrophysiological changes during adolescence: A review," *Brain Cogn.*, vol. 72, no. 1, pp. 86–100, 2010.

[24] A. H. Phan, P. Tichavsky, and A. Cichocki, "CANDECOMP/PARAFAC decomposition of high-order tensors through tensor reshaping," *IEEE Trans. Signal Process.*, vol. 61, no. 19, pp. 4847–4860, oct 2013.